

Role of gluons in soft and semi-hard multiple hadron production in pp collisions at LHC

V.A.Bednyakov¹, A.A.Grinyuk¹, G.I.Lykasov^{1,4}, M.Poghosyan^{2,3}

¹ *JINR, Dubna, Moscow region, 141980, Russia,*

² *Università di Torino/INFN, 10125 Torino, Italy*

³ *CERN, Geneva, Switzerland*

⁴ *E-mail: lykasov@jinr.ru*

Abstract

Hadron inclusive spectra in pp collisions are analyzed within the modified quark-gluon string model including both the longitudinal and transverse motion of quarks in the proton in the wide region of initial energies. The self-consistent analysis shows that the experimental data on the inclusive spectra of light hadrons like pions and kaons at ISR energies can be satisfactorily described at transverse momenta not larger than 1-2 GeV/c. We discuss some difficulties to apply this model at energies above the ISR and suggest to include the distribution of gluons in the proton unintegrated over the internal transverse momentum. It leads to an increase in the inclusive spectra of hadrons and allows us to extend the satisfactory description of the data in the central rapidity region at energies higher than ISR.

1. Introduction

A rather successful description of various characteristics of hadroproduction processes at not large transfer can be obtained by using the approach for describing the soft hadron-nucleon, hadron-nucleus and nucleus-nucleus interactions at high energies based on the topological $1/N$ expansion in QCD [1, 2], where N is the number of flavours or colours, for example, the quark-gluon string model (QGSM) [3, 4], the VENUS model [5], the dual parton model (DPM) [6, 7], the coloured-tube models [8, 9] and others. The conventional QGSM and DPM models used the parton distribution functions (PDF) and the fragmentation functions (FF) integrated over the internal transverse momenta of partons. The modification of the QGSM including the transverse motion of quarks in the initial hadron has been developed in [10] and [11, 12]. It allowed us to describe the inclusive spectra of hadrons produced in pp collisions as a function of the Feynman variable x and the hadron transverse momentum p_t . However, up to now there has not been a self-consistent analysis of these spectra within the QGSM in the wide region of initial energies from the ISR to the LHC ones. In this paper we present the results of the detailed analysis of the inclusive spectra of light hadrons like pions and kaons produced in pp collisions at ISR energies within the modified QGSM including the internal transverse motion of partons in the initial proton. Then we analyze similar spectra of charged hadrons produced in central pp collisions at initial energies from 500 GeV up to 7

TeV and compare them with the $Spp\bar{p}S$, Tevatron and latest LHC data. We discuss some difficulties to apply the modified QGSM to the description of the latest data. To avoid these difficulties we suggest to include the so-called unintegrated gluon distributions in the proton by analyzing soft hadron production in pp collisions at very high energies.

As is well known, hard processes involving incoming protons, such as deep-inelastic lepton-proton scattering (DIS), are described using the scale-dependent PDFs. A distribution like this is usually calculated as a function of the longitudinal momentum fraction x and the square of the four-momentum transfer $q^2 = -Q^2$, integrated over the parton transverse momentum k_t . However, for semi-inclusive processes, such as inclusive jet production in DIS, electroweak boson production [13], etc., the parton distributions unintegrated over the transverse momentum k_t are more appropriate. The theoretical analysis of the unintegrated quark and gluon PDFs can be found, for example, in [14, 15]. According to [15], the gluon distribution function $g(k_t)$ at fixed Q^2 has the very interesting behaviour at small $x \leq 0.01$, it increases very fast starting from almost zero values of k_t . In other words, $g(k_t)$ in some sense blows up when k_t increases and then it decreases at k_t close to 100 GeV/ c . In contrast, the quark distribution $q(k_t)$ is almost constant in the whole region of k_t up to $k_t \sim 100$ GeV/ c and much smaller than $g(x)$. This parametrization of the PDFs was obtained in [15] within the leading order (LO) and next-to-leading order of QCD (NLO) at $Q^2 = 10^2$ (GeV/ c)² and $Q^2 = 10^4$ (GeV/ c)² from the known (DGLAP-evolved [16]) parton densities determined from the global data analysis. At small values of Q^2 the nonperturbative effects should be included to get the PDFs. The nonperturbative effects can arise from the complex structure of the QCD vacuum, see for example [17]-[19]. For example, the instantons are some of the well-studied topological fluctuations of the vacuum gluon fields, see for example [20]-[22] and references therein. In particular, it is shown [22] that the inclusion of the instantons results in the anomalous chromomagnetic quark-gluon interaction (ACQGI) which, for the massive quarks, gives the spin-flip part of it. Within this approach the very fast increase of the unintegrated gluon distribution function at $0 \leq k_t \leq 0.5$ GeV/ c and $Q^2 = 1$ GeV/ c is also shown. These results stimulated us to assume, that the unintegrated gluon distribution in the proton can be included by analyzing also the soft hadron production in pp collisions. We discuss this possibility at the end of this paper.

2. Inclusive spectra of hadrons in pp collisions

2.1 QGSM

Let us analyze the hadron production in pp collisions within the QGSM [3, 4] or the dual parton model (DPM) [6, 7] including the transverse motion of quarks and di-quarks in colliding protons [11, 12]. As is known, the cylinder-type graphs presented in Fig.1 make the main contribution to this process. The physical meaning of the

graph presented in Fig.1 is the following. The left diagram of Fig.1, the so-called one-cylinder graph, corresponds to the case when two colorless strings are formed between the quark/diquark (q/qq) and the diquark/quark (qq/q) in colliding protons, then, after their break, $q\bar{q}$ pairs are created and fragmented to a hadron. The right diagram of Fig.1, the so called multi-cylinder graph, corresponds to a creation of the same two colourless strings and many strings between sea quarks/antiquarks q/\bar{q} and sea antiquarks/quarks \bar{q}/q in the colliding protons. The general form for

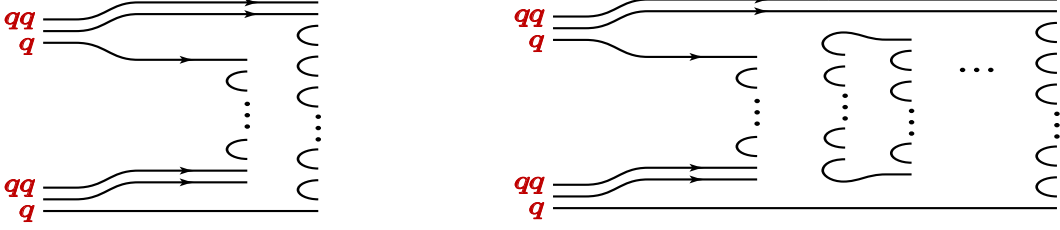


Figure 1: The one-cylinder graph (left) and the multicylinder graph (right) for the inclusive $pp \rightarrow hX$ process.

the invariant inclusive hadron spectrum within the QGSM is the following [3, 4, 23]:

$$E \frac{d\sigma}{d^3\mathbf{p}} \equiv \frac{2E^*}{\pi\sqrt{s}} \frac{d\sigma}{dx dp_t^2} = \sum_{n=1}^{\infty} \sigma_n(s) \phi_n(x, p_t) , \quad (1)$$

where E, \mathbf{p} are the energy and three-momentum of the produced hadron h in the l.s. of colliding protons respectively; E^*, s are the energy of h and the square of the initial energy in the c.m.s of pp ; x, p_t are the Feynman variable and the transverse momentum of h ; σ_n is the cross section for production of the n -pomeron chain (or $2n$ quark-antiquark strings) decaying into hadrons, calculated within the ‘‘eikonal approximation’’ [24], see Appendix; the function $\phi_n(x, p_t)$ has the following form [11] and [25]-[28]:

$$\phi_n(x, p_t) = \int_{x^+}^1 dx_1 \int_{x_-}^1 dx_2 \psi_n(x, p_t; x_1, x_2) , \quad (2)$$

where

$$\begin{aligned} \psi_n(x, p_t; x_1, x_2) = & F_{qq}^{(n)}(x_+, p_t; x_1) F_{q_v}^{(n)}(x_-, p_t; x_2) / F_{q_v}^{(n)}(0, p_t) + \\ & + F_{q_v}^{(n)}(x_+, p_t; x_1) F_{qq}^{(n)}(x_-, p_t; x_2) / F_{qq}^{(n)}(0, p_t) + \\ & 2(n-1) F_{q_s}^{(n)}(x_+, p_t; x_1) F_{\bar{q}_s}^{(n)}(x_-, p_t; x_2) / F_{q_s}^{(n)}(0, p_t) . \end{aligned} \quad (3)$$

and $x_{\pm} = 0.5(\sqrt{x^2 + x_t^2} \pm x)$, $x_t = 2\sqrt{(m_h^2 + p_t^2)/s}$,

$$F_{\tau}^{(n)}(x_{\pm}, p_t; x_{1,2}) = \int d^2k_t \tilde{f}_{\tau}^{(n)}(x_{\pm}, k_t) \tilde{G}_{\tau \rightarrow h} \left(\frac{x_{\pm}}{x_{1,2}}, \tilde{k}_t; p_t \right) , \quad (4)$$

$$F_\tau^{(n)}(0, p_t) = \int_0^1 dx' d^2 k_t \tilde{f}_\tau^{(n)}(x', k_t) \tilde{G}_{\tau \rightarrow h}(0, p_t) = \tilde{G}_{\tau \rightarrow h}(0, p_t) . \quad (5)$$

Here τ means the flavour of the valence (or sea) quark or diquark, $\tilde{f}_\tau^{(n)}(x', k_t)$ is the quark distribution function depending on the longitudinal momentum fraction x' and the transverse momentum k_t in the n -pomeron chain; $\tilde{G}_{\tau \rightarrow h}(z, \tilde{k}_t; p_t) = z \tilde{D}_{\tau \rightarrow h}(z, \tilde{k}_t; p_t)$, $\tilde{D}_{\tau \rightarrow h}(z, \tilde{k}_t; p_t)$ is the fragmentation function of a quark (antiquark) or diquark of flavour τ into a hadron h . We present the quark distribution in a proton in the factorized form $\tilde{f}_\tau(x, k_t) = f_\tau(x)g_\tau(k_t)$, and choose the k_t distribution of quarks and the FF in the simple Gaussian form $g(k_t) = (\gamma_q/\pi)\exp(-\gamma_q k_t^2)$, $g_{q \rightarrow h}(\tilde{k}_t) = (\gamma_F/\pi)\exp(-\gamma_F \tilde{k}_t^2)$, where $\tilde{k}_t = p_t - z k_t$, $z = x_\pm/x_{1,2}$. Then, the quark functions in the n -pomeron chain will be factorized too [11]

$$\tilde{f}_\tau^{(n)}(x, k_t) = f_\tau^{(n)}(x)g_\tau^{(n)}(k_t) , \quad (6)$$

where

$$g_\tau^{(n)}(k_t) = \frac{\gamma_n}{\pi} \exp(-\gamma_n k_t^2), \quad \gamma_n = \frac{\gamma_q}{n} . \quad (7)$$

The fragmentation function also reads

$$\tilde{G}_{\tau \rightarrow h}(z, \tilde{k}_t; p_t) = G_{\tau \rightarrow h}(z, p_t)g_{\tau \rightarrow h}(\tilde{k}_t) . \quad (8)$$

Then, substituting Eqs.(6) into Eq.(4) we get the following form for $F_\tau^{(n)}$:

$$F_\tau^{(n)}(x_\pm, p_t; x_{1,2}) = f_\tau^{(n)}(x_{1,2})G_{\tau \rightarrow h}(z)\tilde{I}_n(z, p_t) , \quad (9)$$

where the function $\tilde{I}_n(z, p_t)$ reads [12, 11]

$$\tilde{I}_n(z, p_t) = \frac{\gamma_z}{\pi} \exp(-\gamma_z p_t^2), \quad \gamma_z = \frac{\gamma_F}{1 + n\rho z^2}, \quad \rho = \frac{\gamma_F}{\gamma_q} . \quad (10)$$

When we take the k_t distribution of quarks (diquarks) $g(k_t)$ and the FF $g_{q \rightarrow h}(\tilde{k}_t)$ in the exponential form

$$g(k_t) = \frac{B_q^2}{2\pi} \exp(-B_q k_t^2) , \quad g_{q \rightarrow h}(\tilde{k}_t) = \frac{B_F^2}{2\pi} \exp(-B_F \tilde{k}_t^2) , \quad (11)$$

we get the following form for the function $I_n(z, p_t)$ entering into $F_\tau^{(n)}(x_\pm, p_t; x_{1,2})$

$$F_\tau^{(n)}(x_\pm, p_t; x_{1,2}) = f_\tau^{(n)}(x_{1,2})G_{\tau \rightarrow h}(z)I_n(z, p_t) , \quad (12)$$

$$I_n(z, p_t) = C_n \int \frac{J_0(bp_t)bdb}{(z^2 b^2 + B_q^2)^{3n/2} (b^2 + B_F^2)^{3/2}} . \quad (13)$$

Here $J_0(bp_t)$ is the zero order Bessel function and the coefficient C_n is determined by the normalization equation

$$\int d^2 p_t I_n(z, p_t) = 1 \quad (14)$$

Equation (14) is similar to the normalization equation for the function $\tilde{I}_n(z, p_t)$ given by Eq.(10), when the quark distributions and the FF are chosen as the Gaussian forms.

• **Gluon distribution in proton .**

As is mentioned in the Introduction, the unintegrated gluon distribution in the proton at small values of x , as a function of k_t , increases very fast when k_t increases and then slowly decreases, according to the instanton vacuum approach for the massive quarks [22] at small $Q^2 \sim 1 \text{ GeV}/c$. The similar behaviour for $g(k_t)$ was obtained within the NLO QCD calculations at large $Q^2 = 10^2 \text{ GeV}/c$ and $Q^2 = 10^4 \text{ GeV}/c$ for the massless quarks [15] and in [29, 30] where the parametrization for the gluon distribution at the starting value Q_0^2 was found as

$$g(k_t, x, Q_0^2) \sim R_0^2(x) k_t^2 \exp(-R_0^2(x) k_t^2) , \quad (15)$$

with the parameters given in [32]. The motivation of the form given by Eq.(15) is based on the saturation model [31]-[33]. Unintegrated gluon distributions were also studied in [14] within the dipole model where the similar qualitative k_t dependence was shown. On the basis of these results we will try to include the contribution of gluons in soft pp collisions.

• **Hadron production in central rapidity region.**

According to the Abramovskiy-Gribov-Kancheli cutting rules (AGK) [34], at mid-rapidity only Mueller-Kancheli type diagrams contribute to the inclusive spectrum of hadrons. In our approach the function $F_\tau^{(n)}$ is calculated in such a way that in the central region ($y = 0$), when $x \simeq 0$ and $z \simeq 0$, it becomes proportional to n and satisfies AK cancellation. Thus,

$$\rho_q(0, p_t) = \phi_q(0, p_t) \sum_{n=1}^{\infty} n \sigma_n(s) = g(s/s_0)^\Delta \phi_q(0, p_t), \quad (16)$$

where $\phi_q(x = 0, p_t)$ depends only on p_t , $s_0 = 1 \text{ GeV}^2$. Considering the gluons from incoming protons, which may split into $q\bar{q}$ pairs, we get an additional contribution to the spectrum

$$\begin{aligned} \rho_g(x = 0, p_t) &= \phi_g(0, p_t) \sum_{n=2}^{\infty} (n-1) \sigma_n(s) \equiv \\ &\phi_g(0, p_t) (g(s/s_0)^\Delta - \sigma_{nd}) , \end{aligned} \quad (17)$$

where $\Delta = 0.12$, $g=21 \text{ mb}$ and σ_{nd} is the cross section of exchange of any number cut-pomerons. The quantities

$$\sum_{n=1}^{\infty} n \sigma_n(s) = g(s/s_0)^\Delta ; \quad \sum_{n=1}^{\infty} \sigma_n(s) = \sigma_{nd} \quad (18)$$

were calculated in [24] within the ‘‘quasi-eikonal’’ approximation [24]. Assuming that one of the cut-pomerons is always stretched between valence quarks and diquarks

which are not coming from the splitting of gluons, in Eq. (9) we excluded unity from n . Finally, we can present the inclusive spectrum at $x \simeq 0$ in the following form:

$$\begin{aligned} \rho(p_t) &= \rho_q(x=0, p_t) + \rho_g(x=0, p_t) = \\ &g(s/s_0)^\Delta \phi_q(0, p_t) + \left(g(s/s_0^\Delta - \sigma_{nd}\right) \phi_g(0, p_t) , \end{aligned} \quad (19)$$

We fix these contributions from the data on the charged particles p_t distribution, parametrizing them as follows:

$$\begin{aligned} \phi_q(0, p_t) &= A_q \exp(-b_q p_t) \\ \phi_g(0, p_t) &= A_g \sqrt{p_t} \exp(-b_g p_t). \end{aligned} \quad (20)$$

The parameters are fixed from the fit to the data on the p_t distribution of charged particles at $y = 0$: $A_q = 0.1912 \pm 0.0064$; $b_q = 7.24 \pm 0.11$ (GeV/c) $^{-1}$ and $A_g = 0.0568 \pm 0.002$; $b_g = 3.46 \pm 0.02$ (GeV/c) $^{-1}$.

2..2 Hard Scattering

As will be shown below, the approach suggested above will be able to describe many data on the inclusive p_t spectra in the central pp collisions at not large values of $p_t \leq 2$ GeV/c. Therefore, at larger p_t we calculate these spectra, which are due to the hard pp collision, within the leading order of perturbative QCD (LOQCD). According to the model of hard scattering [45]-[53], the relativistic invariant inclusive spectrum of the hard process $p + p \rightarrow h + X$ can be related to the elastic parton-parton subprocess $i + j \rightarrow i' + j'$, where i, j are the partons (quarks and gluons). This spectrum can be presented in the following general form [47]-[49]:

$$\begin{aligned} \rho(x, p_t)_{hard} &\equiv E \frac{d\hat{\sigma}_{hard}}{d^3p} = \sum_{i,j} \int d^2k_{it} \int d^2k_{jt} \int_{x_i^{min}}^1 dx_i \int_{x_j^{min}}^1 dx_j \\ &\int_0^1 dz f_i(x_i, k_{it}) f_j(x_j, k_{jt}) \frac{\hat{s}}{\pi} \frac{d\sigma_{ij}(\hat{s}, \hat{t})}{d\hat{t}} \frac{1}{z^2} D_{i,j}^h(z) \delta(\hat{s} + \hat{t} + \hat{u}) \end{aligned} \quad (21)$$

where $s = (p_1 + p_2)^2 \simeq 2p_1 \cdot p_2$, p_1, p_2 are the four-momenta of the colliding protons. In the c.m.s. of pp (LHC facility, when $\vec{p}_1 = -\vec{p}_2$) $s = 4E_1^2$, i.e., $E_1 = \sqrt{s}/2$; $t = (p_1 - p_h)^2 \simeq -2p_1 \cdot p_h = -2(E_1 E_h - \vec{p}_1 \vec{p}_h)$; $u = (p_2 - p_h)^2 \simeq -2p_2 \cdot p_h = -2(E_1 E_h - \vec{p}_1 \vec{p}_h)$; $x_{(i,j)} = 2k_{(i,j)z}/\sqrt{s}$; $E_{(1,2,h)} = \sqrt{m_{(1,1,h)}^2 + \vec{p}_{(1,2,h)}^2}$, $\vec{p}_{(1,2,h)}$ are the three-momenta of hadrons 1, 2, h respectively; $k_{(i,j)z}$ are the longitudinal momenta (relative to \vec{p}_A) of the partons i or j in the pp c.m.s., z is the fraction of the hadron momentum from the parton momentum, $f_{i,j}$ is the PDF, whereas $D_{i,j}$ is the FF, $\hat{s}, \hat{t}, \hat{u}$ are the Mandelstam variables for the parton-parton elastic scattering, see the details in [47]. Calculating Eq.(22) we used the PDF, FF and $d\sigma_{ij}(\hat{s}, \hat{t})/d\hat{t}$ obtained within LO QCD [50]-[53].

3. Results and discussion

In Figs.(2-5) we illustrate how our approach works for the description of the experimental data on the inclusive spectra of pions and kaons produced in pp collisions when we neglect the gluon distributions in the proton. It allows a satisfactory description of these spectra as functions of x and p_t , up to $p_t = 1.4$ GeV/ c at the initial ISR energies $\sqrt{s} = 23.3 - 53$ GeV. The ISR experimental data presented in Figs.(2-5) are taken from [35]. The quark (diquark) distribution and the FF as a function of the internal transverse momentum k_t and \tilde{k}_t are chosen in the exponential form given by Eq.(11). We took the same parameters B_q and B_F for all the initial ISR energies, namely $B_q = 4.5$ GeV/ c for both valence and sea quarks of any flavour and $B_F = 2.8$ GeV/ c for π^\pm and $B_F = 2.4$ GeV/ c for K^\pm mesons. Figures (2-5) show that the modified QGSM results in a self-consistent satisfactory description of the inclusive spectra of light mesons produced in pp collisions at ISR energies at different values of x and p_t not larger than 1.5 GeV/ c . However, one cannot satisfactorily describe similar spectra at the $Spp\bar{S}$, Tevatron and LHC energies ignoring the gluon contribution .

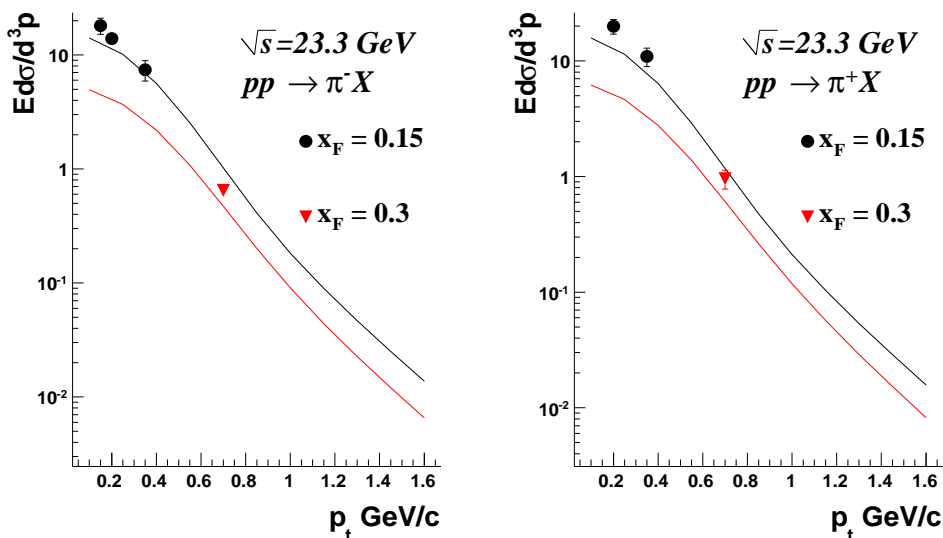


Figure 2: The inclusive spectrum $E d\sigma/d^3p$ [mbGeV $^{-2}$ c 3] of π^- mesons (left) produced in pp collision at $\sqrt{s} = 23.3$ GeV; the similar spectrum but for π^+ mesons (right).

The result of the fit to data using Eq.(20) on the charged hadron inclusive spectra is presented in Figs.(7,8). The long-dash curve corresponds to the quark contribution $\rho_q(x = 0, p_t)$ given by Eq.(16), and the short-dash line is the gluon contribution $\rho_g(x = 0, p_t)$ (Eq.17) to the invariant yield $d^3N/dy d^2p_t$; the solid curve corresponds to the sum of both contributions, see Eqs.(19,20). One can see that the conventional

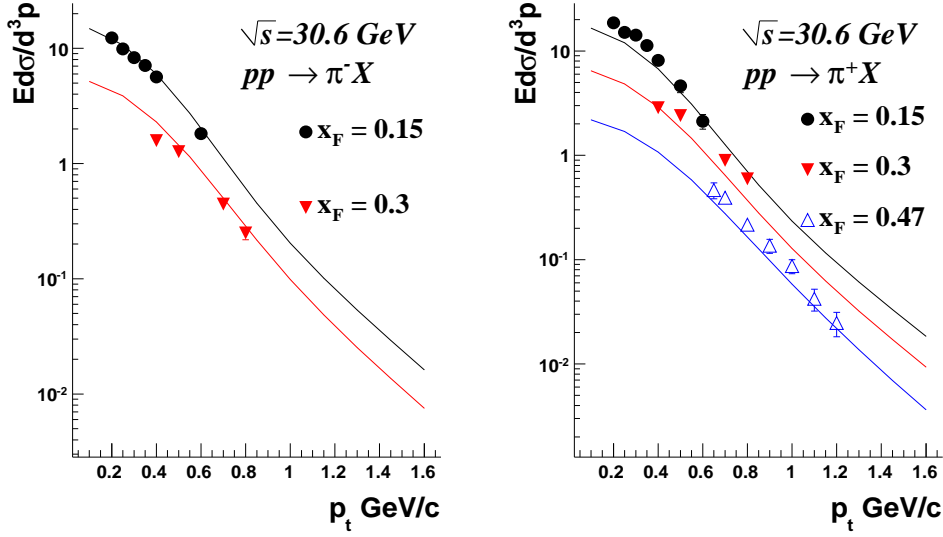


Figure 3: The inclusive spectrum $Ed\sigma/d^3p$ [mbGeV $^{-2}c^3$] of π^- mesons (left) produced in pp collision at $\sqrt{s} = 30.6$ GeV; the similar spectrum but for π^+ mesons (right).

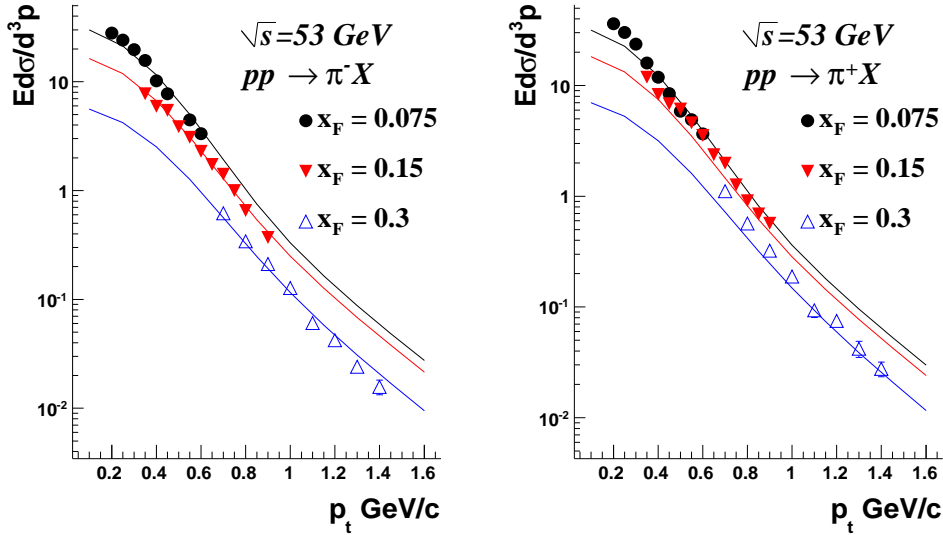


Figure 4: The inclusive spectrum $Ed\sigma/d^3p$ [mbGeV $^{-2}c^3$] of π^- mesons (left) produced in pp collision at $\sqrt{s} = 53$ GeV; the similar spectrum but for π^+ mesons (right).

quark contribution $\Phi^q(y = 0, p_t)$ is able to describe the data up to $p_t \leq 1$ GeV/ c ,

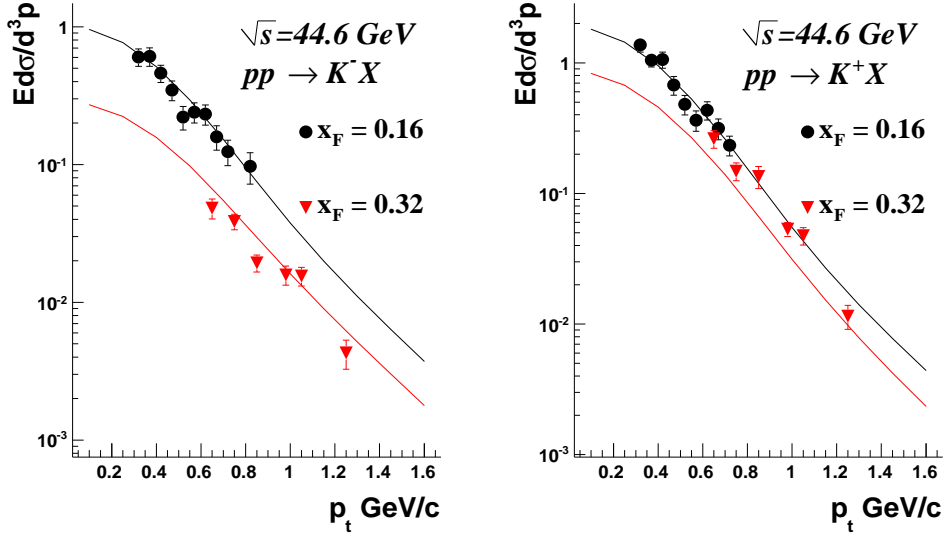


Figure 5: The inclusive spectrum $Ed\sigma/d^3p$ [$\text{mbGeV}^{-2}\text{c}^3$] of K^- mesons (left) produced in pp collision at $\sqrt{s} = 44.6$ GeV; the similar spectrum but for K^+ mesons (right).

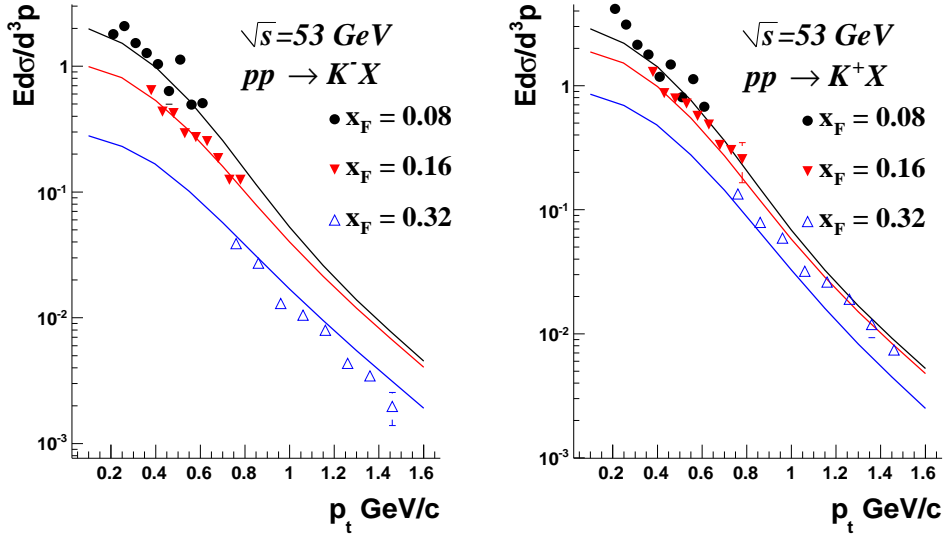


Figure 6: The inclusive spectrum $Ed\sigma/d^3p$ [$\text{mbGeV}^{-2}\text{c}^3$] of K^- mesons (left) produced in pp collision at $\sqrt{s} = 53$ GeV; the similar spectrum but for K^+ mesons (right).

whereas the inclusion of the gluon contribution allows us to extend the range of

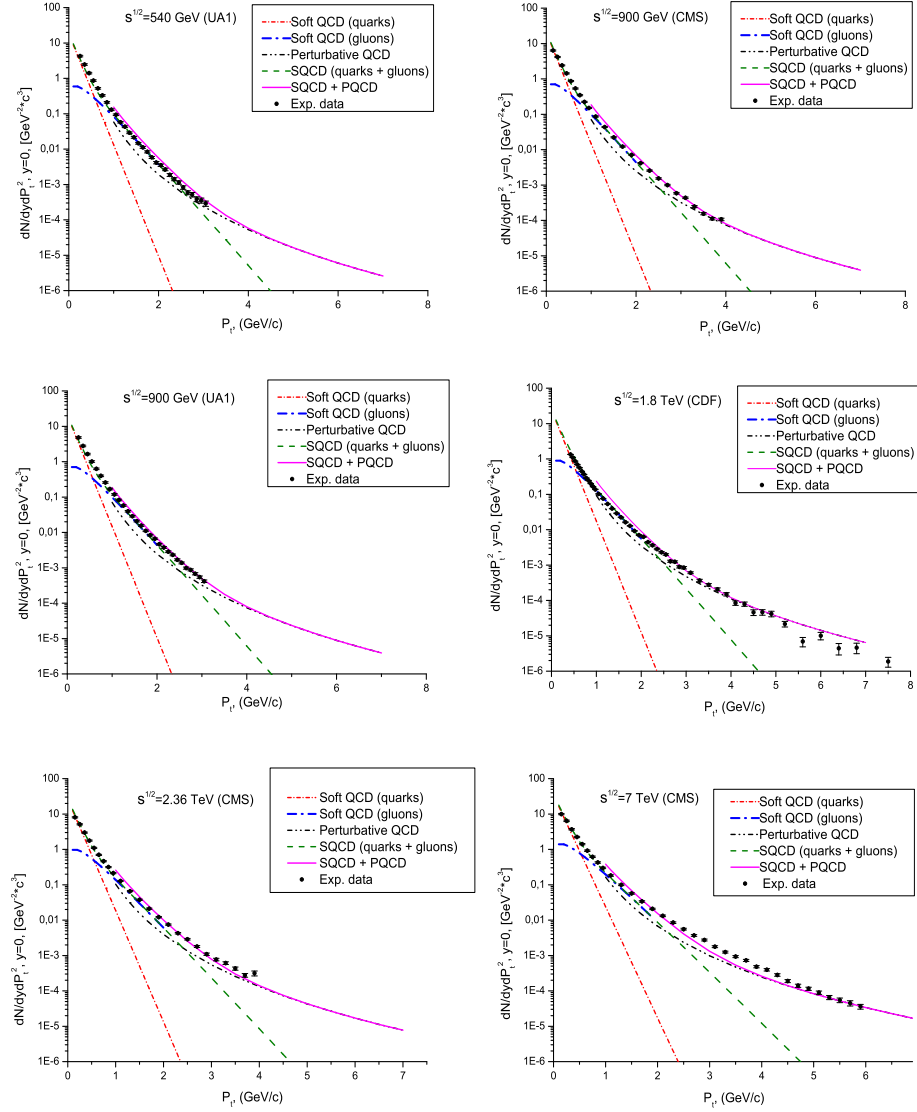


Figure 7: The inclusive spectrum of the charged hadron as a function of p_t (GeV/c) in the central rapidity region ($y = 0$) at $\sqrt{s} = 540, 900$ GeV (top) and $\sqrt{s} = 1.8, 2.36, 7$ TeV. The data are taken from [36, 37, 38].

good description up to 2 GeV/c. At larger values of p_t the contribution of hard processes is not negligible and one has to take them into account on the basis of

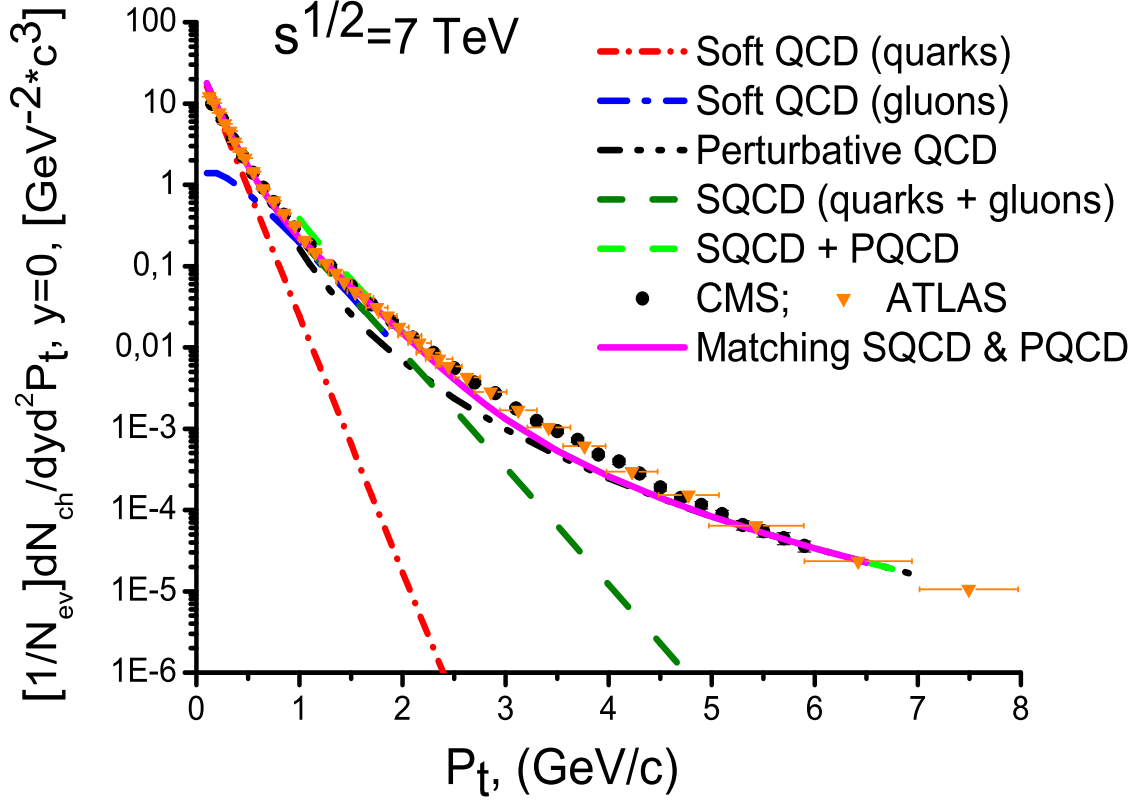


Figure 8: The inclusive spectrum of the charged hadron as a function of p_t (GeV/c) in the central rapidity region ($y = 0$) at $\sqrt{s} = 7$ TeV compared with the CMS [38] and ATLAS [39] data.

the perturbative QCD. Figure 7 also shows that, according to the experimental data, the shape of the inclusive p_t spectrum at $y = 0$ slowly changes as the initial energy increases. Its p_t dependence appears harder as the energy increases. It is probably due to the jet production which occurs even at not large values of p_t when \sqrt{s} increases. In Fig.8 the same results as in Fig.7(right, bottom) except the solid line are presented. The solid line in Fig.8 corresponds to the matching of the calculations obtained within the soft QCD (SQCD) and perturbative QCD (PQCD). The SQCD means our calculations within the QGSM including the gluons in the proton, see Eq.(19) In Fig.9 the ratio of our calculations to the experimental data [38] at $\sqrt{s} = 900$ GeV (top) and $\sqrt{s} = 7$ TeV are presented. It is shown that the discrepancy between theoretical results and the experimental data is less than 30 percent at $p_t \leq 2$.GeV/c.

The effective inclusion of the unintegrated distributions of gluons in the proton [29, 30] allows us to extend the satisfactory description of the experimental data

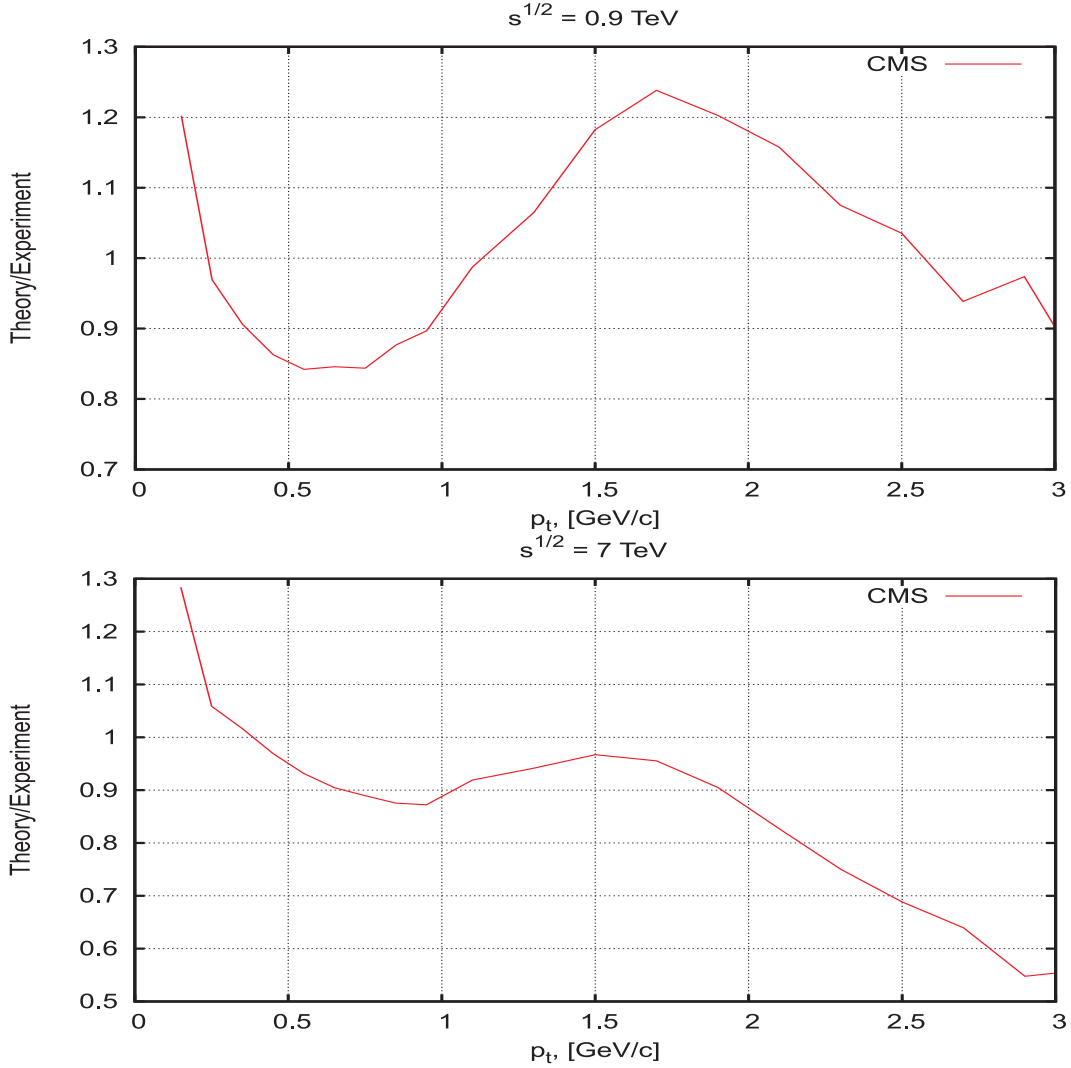


Figure 9: The ratio of our calculations of the inclusive p_t spectrum as a function of p_t (GeV/c) in the central rapidity region ($y = 0$) to the corresponding experimental data at $\sqrt{s} = 900$ GeV (top) and $\sqrt{s} = 7$ TeV (bottom). The data are taken from [38].

on the inclusive spectra of charged hadrons at $y = 0$ up to $p_t \sim 2\text{GeV}/c$. At higher values of the transverse momentum we include hard pp collision calculated within LO QCD [45]-[53]. Parton interactions should be considered for describing the experimental data. These results are presented in Figs.(7,8) at $p_t > 2\text{GeV}/c$.

4. Conclusion

Our study has shown that soft QCD or the modified QGSM including both the longitudinal and transverse motion of partons in the proton is able to describe

rather satisfactorily the experimental data on inclusive spectra of light hadrons like pions and kaons produced in pp collisions at the ISR energies and at not large values of the transverse momenta $p_t \leq 1.4 - 1.5 \text{ GeV}/c$. These calculations were made in the self-consistent way, i.e., the parameters entering into the quark distribution and the FF, as a function of the internal transverse momentum, are the same at all the initial energies \sqrt{s} up to about a few hundred GeV. The conventional QGSM or DPM model does not include the distribution of gluons in the proton. However, as is well known, at large transverse momenta p_t of hadrons the gluons in the proton play a very important role in description of the experimental data. Therefore, one can assume that the contribution of the gluon distribution in the proton to the inclusive spectrum of produced hadrons slowly appears when p_t increases and it will be sizable at high values of p_t . This assumption is also confirmed by the increase of the unintegrated gluon distribution in the proton at $x \sim 0$ as a function of the internal transverse momentum k_t when k_t grows [15, 22, 29].

Therefore, to illustrate this hypothesis we fit the experimental data on the inclusive spectra of charged particles produced in the central pp collisions at energies larger than the ISR starting from 500 GeV up to 7 TeV by the sum of the quark contribution ρ_q given by Eq.(16) and the gluon contribution ρ_g (see Eq.(18)). The parameters of this fit do not depend on the initial energy in that energy interval. This fit shows that the inclusion of only the quark contribution ρ_q allows us to describe the data at $y = 0$ up to $p_t \sim 1 \text{ GeV}/c$, while the inclusion of the gluon contribution ρ_g results in a satisfactory description of the data up to $p_t \simeq 2 \text{ GeV}/c$. The inclusion of the hard pp collision within LO QCD allows us to describe rather satisfactorily the data in the wide region of p_t .

Acknowledgements

The authors are very grateful to A.Bakulev, V.Cavazini, A.Dorokhov, A.V.Efremov, F.Francavilla, C. Gwenlan, H.Jung, V.Kim, B.Kniehl, N.Kochelev, E.A.Kuraev, L.N.Lipatov, T.Lomtadze, M.Mangano, C.Merino, S.V.Mikhailov, E.Nurse, F.Palla, E.Pilkington, A.F.Pikelner, C.Royon, M.G.Ryskin, E.Sarkisyan-Grinbaum, O.V.Teryaev, Yu.Shabelski and V.V.Uzhinskiy for very useful discussions and comments. This work was supported in part by the Russian Foundation for Basic Research, project No:11-02-01538-a.

5. Appendix

• Quark distributions in proton within QGSM

Let us present the quark distributions in a proton obtained within the Regge theory in Refs.[3, 4, 23]. The distributions for valence u and d quarks in the n chain (see Fig.1) read

$$f_{u_v}^{(n)}(x) = C_u x^{-\alpha_R(0)} (1-x)^{\alpha_R(0)-2\alpha_N(0)+n-1}, \quad f_{d_v}^{(n)}(x) = f_{u_v}^{(n)}(x) \cdot (1-x). \quad (22)$$

There are the following relations for the sea u and d quarks:

$$f_{u_{sea}}^{(n)}(x) = f_{\bar{u}_{sea}}^{(n)}(x) = f_{u_v}^{(n)}(x) ; f_{d_{sea}}^{(n)}(x) = f_{\bar{d}_{sea}}^{(n)}(x) = f_{d_v}^{(n)}(x) . \quad (23)$$

For the charmed quarks $c\bar{c}$ in a proton we have [12]

$$f_{c\bar{c}}^{(n)}(x) = C_{c\bar{c}} x^{\alpha_\psi(0)} (1-x)^{2(\alpha_R(0)-\alpha_N(0))-\alpha_\psi(0)+n-1} \quad (24)$$

The distributions of the diquarks ud and uu in a proton read

$$f_{ud}^{(n)}(x) = C_{ud} x^{\alpha_R(0)-2\alpha_N(0)} (1-x)^{-\alpha_R(0)+n-1} ; f_{uu}^{(n)}(x) = f_{ud}^{(n)}(x) \cdot (1-x) . \quad (25)$$

Here $\alpha_R(0), \alpha_N(0)$ and $\alpha_\psi(0)$ are the intercepts of the Reggeon, nucleon and ψ Regge trajectories. As is well known (see, for example, [23]), $\alpha_R(0) = 0.5$ and $\alpha_N(0) \simeq -0.5$. The value for the intercept of the ψ Regge trajectory is known not so well because Regge trajectories of heavy mesons can be nonlinear as functions of the transfer t . For the linear ψ Regge trajectory $\alpha_\psi(0) = -2.18$, whereas for the nonlinear $\psi(t)$ the intercept value can be about zero, $\alpha_\psi(0) = 0$ [41]. The coefficients C_i in Eqs.(22-25) are determined by the normalization condition

$$\int_0^1 f_i^{(n)}(x) dx = 1 . \quad (26)$$

• **Fragmentation functions of quarks (diquarks) to π mesons within QGSM**

The fragmentation functions of quarks (diquarks) to π mesons $G_{q(qq)\rightarrow\pi}(z) = z D_{q(qq)\rightarrow\pi}$ have the following forms [23, 40, 42]:

$$G_{u\rightarrow\pi^+}(z) = a_0(1-z)^{\alpha_R(0)+\lambda} ; G_{u\rightarrow\pi^-}(z) = (1-z)G_{u\rightarrow\pi^+} , \quad (27)$$

$$G_{d\rightarrow\pi^+}(z) = G_{u\rightarrow\pi^-}(z) , G_{d\rightarrow\pi^-}(z) = G_{u\rightarrow\pi^+}(z) , \quad (28)$$

$$G_{uu\rightarrow\pi^+}(z) = a_0(1-z)^{\alpha_R(0)-2\tilde{\alpha}_B(0)+\lambda} ; G_{uu\rightarrow\pi^-}(z) = (1-z)G_{uu\rightarrow\pi^+}(z) , \quad (29)$$

$$G_{ud\rightarrow\pi^+}(z) = G_{ud\rightarrow\pi^-}(z) = a_0 \left(1 + (1-z)^2\right) (1-z)^{\alpha_R(0)-2\tilde{\alpha}_B(0)+\lambda} \quad (30)$$

and

$$G_{dd\rightarrow\pi^-}(z) = G_{uu\rightarrow\pi^+}(z) ; G_{dd\rightarrow\pi^+}(z) = G_{uu\rightarrow\pi^-}(z) . \quad (31)$$

In the above equations $\alpha_R(0) = 0.5, \tilde{\alpha}_B(0) = -0.5, a_0 = 0.65$ and $\lambda = 2\alpha'_R(0) < p_t^2 > \simeq 0.5, \alpha'_R(0)$ and $< p_t^2 >$ being the slope of the Regge trajectory and the mean value of the Tahoe transverse hadron momentum squared.

• **FF for K^\pm mesons within QGSM**

The FFs for K^\pm mesons are [43]

$$G_{u\rightarrow K^+}(z) = G_{d\rightarrow K^0}(z) = a_K(1-z)^{-\alpha_\phi(0)+\lambda}(1+a_{1K}z) , \quad (32)$$

$$G_{u \rightarrow K^-}(z) = G_{d \rightarrow \bar{K}^0}(z) = G_{d \rightarrow \bar{K}^+}(z) = G_{u \rightarrow K^0}(z) = G_{d \rightarrow \bar{K}^-}(z) = G_{d \rightarrow \bar{K}^0}(z a_K (1-z)^{-\alpha_\phi(0)+\lambda+1}, \quad (33)$$

$$G_{\bar{u} \rightarrow K^-}(z) = G_{u \rightarrow K^+}(z), \quad G_{\bar{u} \rightarrow K^+}(z) = G_{u \rightarrow K^-}(z), \quad (34)$$

$$G_{\bar{d} \rightarrow K^-}(z) = G_{d \rightarrow K^+}(z), \quad G_{\bar{d} \rightarrow K^+}(z) = G_{d \rightarrow K^-}(z),$$

$$G_{\bar{s} \rightarrow K^0}(z) = G_{\bar{s} \rightarrow \bar{K}^+}(z) = G_{s \rightarrow K^-}(z) = G_{s \rightarrow \bar{K}^0}(z) = b_K z^{1-\alpha_\phi(0)} (1-z)^{-\alpha_R(0)+\lambda} + a_K (1-z)^{-\alpha_R(0)+\lambda+2(1-\alpha_\phi(0))} \quad (35)$$

$$G_{\bar{s} \rightarrow K^-}(z) = G_{\bar{s} \rightarrow \bar{K}^0}(z) = G_{s \rightarrow K^+}(z) = G_{s \rightarrow \bar{K}^0}(z) = a_K (1-z)^{-\alpha_R(0)+\lambda+2(1-\alpha_\phi(0))} \quad (36)$$

$$G_{uu \rightarrow K^+}(z) = a_K (1-z)^{2\alpha_R(0)-\alpha_\phi(0)-2\alpha_N(0)+\lambda} (1+a_{2K}z), \quad (37)$$

$$G_{ud \rightarrow K^+}(z) = \frac{a_K}{2} (1-z)^{2\alpha_R(0)-\alpha_\phi(0)-2\alpha_N(0)+\lambda} (1+a_{2K}z + (1-z)^2), \quad (38)$$

$$G_{uu \rightarrow K^-}(z) = G_{uu \rightarrow K^0}(z) = G_{uu \rightarrow \bar{K}^0}(z) a_K (1-z)^{-\alpha_\phi(0)-2\alpha_N(0)+\lambda+2}, \quad (39)$$

$$G_{ud \rightarrow K^-}(z) = G_{ud \rightarrow \bar{K}^0}(z) = \frac{a_K}{2} (1-z)^{-\alpha_\phi(0)-2\alpha_N(0)+\lambda+2} (1+(1-z)^2), \quad (40)$$

$$G_{ud \rightarrow K^0}(z) = \frac{a_K}{2} (1-z)^{-\alpha_\phi(0)-2\alpha_N(0)+\lambda+2} (2+a_{2K}z), \quad (41)$$

Here $\lambda = 2\alpha' \bar{p}_t^2 \simeq 0.5$, $\alpha_R(0) = 0.5$, $\alpha_N(0) \simeq -0.5$, $a_{1K} = 2$, $a_{2K} = 5$, $b_K = 0.4$.

• **FF for p and \bar{p} within QGSM**

Now, the FFs for protons p and antiprotons \bar{p} are [44]

$$G_{u \rightarrow p}(z) = a_{\bar{p}} (1-z)^{\alpha_R(0)-2\alpha_N(0)+\lambda}; \quad G_{u \rightarrow \pi^-}(z) = (1-z) G_{u \rightarrow \pi^+}, \quad (42)$$

$$G_{d \rightarrow p}(z) = \frac{a_{\bar{p}}}{3} (1-z)^{\alpha_R(0)-2\alpha_N(0)+\lambda} (3-z); \quad (43)$$

$$G_{uu \rightarrow p}(z) = G_{1uu \rightarrow p}(z) + G_{2uu \rightarrow p}(z), \quad (44)$$

$$G_{1uu \rightarrow p}(z) = a_p z^{2(\alpha_R(0)-\alpha_N(0))} (1-z)^{-\alpha_R(0)+\lambda} (3-2z), \quad (45)$$

$$G_{2uu \rightarrow p}(z) = a_p (1-z)^{-\alpha_R(0)+\lambda+4(1-\alpha_N(0))}, \quad (46)$$

$$G_{1ud \rightarrow p}(z) = a_p z^{2(\alpha_R(0) - \alpha_N(0))} (1 - z)^{-\alpha_R(0) + \lambda} , \quad (47)$$

$$G_{2ud \rightarrow p}(z) = G_{2uu \rightarrow p}(z) , \quad G_{u \rightarrow \bar{p}}(z) = G_{\bar{u} \rightarrow p}(z) = G_{d \rightarrow \bar{p}}(z) = \quad (48)$$

$$G_{\bar{d} \rightarrow p}(z) = G_{\bar{u} \rightarrow p}(z) = a_{\bar{p}} (1 - z)^{-\alpha_R(0) + 2(1 - \alpha_N(0)) + \lambda} \quad (49)$$

$$G_{uu \rightarrow \bar{p}}(z) = G_{ud \rightarrow \bar{p}}(z) = a_{\bar{p}} (1 - z)^{\alpha_R(0) - 2\alpha_N(0) + 2(1 - \alpha_N(0)) + \lambda} \quad (50)$$

$$G_{\bar{u} \rightarrow \bar{p}}(z) = G_{\bar{d} \rightarrow \bar{p}}(z) = G_{u \rightarrow p}(z) . \quad (51)$$

Here $\alpha_p(0) = 0.9$ and $\alpha_{\bar{p}}(0) = 0.07$.

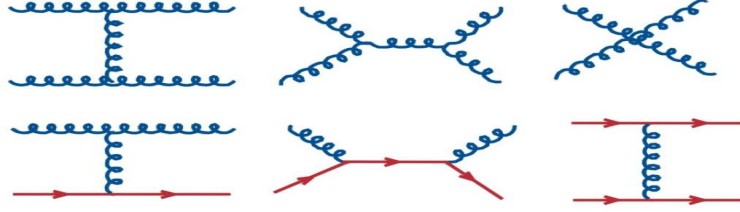
• Hard scattering

Present now the scheme for the calculations of the differential cross section of the parton-parton elastic scattering within the LO QCD. Figure 9 (top) illustrates the parton-parton scattering within the LO QCD. In Fig.9 (middle and bottom) the differential parton-parton cross sections calculated within the LO QCD are presented [50]. Here Λ is the chromodynamic constant which has taken from [52, 53], n_f is the number of flavours, A_1 is the dimensional coefficient to get the dimension $\text{mb}/(\text{GeV}/c)^2$ for $d\sigma_{ij}/d\hat{t}$. The four-momentum transfer squared Q^2 is related to the Mandelstam variables $\hat{s}, \hat{t}, \hat{u}$ for the elastic parton-parton scattering [49]

$$Q^2 = \frac{2\hat{s}\hat{t}\hat{u}}{\hat{s}^2 + \hat{t}^2 + \hat{u}^2} . \quad (52)$$

References

- [1] G. t'Hooft, Nucl.Phys. **B72** (1974) 461.
- [2] M. Ciafaloni, G. Marchesini and G. Veneziano, Nucl.Phys. **B98** (1975) 472.
- [3] A. B. Kaidalov, Phys.Lett. **B116** (1982) 459.
- [4] A. B. Kaidalov and K. A. Ter-Martirosyan, Phys.Lett. **B 117** (1982) 247.
- [5] K. Werner, Phys.Rep.**232** (1993) 87.
- [6] A.Capella, J,Tran Thanh Van, Phys.Lett., **114B**, 450 (1982);
- [7] A.Capella, U.Sukhatme, C.J.Tan, J,Tran Thanh Van, Phys.Rev. **D36**, 109 (1987); *ibid* Adv.Ser.Direct.High Energy Phys.2:428-480,1988.
- [8] A. Casher, J. Kogut, and L. Susskind, Phys.Rev. **D10** (1974) 732.
- [9] E. G. Gurvich, Phys.Lett. **B87** (1979) 386.



Parton - parton interactions within LO QCD,
the wavy line is the gluon, the solid line is the quark.

$$\frac{d\sigma_{ij}}{d\hat{t}} = \frac{8\pi}{\hat{s}} A_1 \alpha_s^2 \frac{d\sigma_{ij}}{d\Phi_2}; \alpha_s(Q^2) = \frac{12\pi}{(33 - 2n_f) \ln(Q^2 / \Lambda^2)};$$

Process	$\frac{d\hat{\sigma}}{d\Phi_2}$	Process	$\frac{d\hat{\sigma}}{d\Phi_2}$
$qq' \rightarrow qq'$	$\frac{1}{2\hat{s}} \frac{4\hat{s}^2 + \hat{u}^2}{9\hat{t}^2}$	$q\bar{q} \rightarrow gg$	$\frac{1}{2} \frac{1}{2\hat{s}} \left[\frac{32\hat{t}^2 + \hat{u}^2}{27\hat{t}\hat{u}} - \frac{8\hat{t}^2 + \hat{u}^2}{3\hat{s}^2} \right]$
$qq \rightarrow qq$	$\frac{1}{2\hat{s}} \frac{1}{2\hat{s}} \left[\frac{4}{9} \left(\frac{\hat{s}^2 + \hat{u}^2}{\hat{t}^2} + \frac{\hat{s}^2 + \hat{t}^2}{\hat{u}^2} \right) - \frac{8\hat{s}^2}{27\hat{u}\hat{t}} \right]$	$gg \rightarrow q\bar{q}$	$\frac{1}{2\hat{s}} \left[\frac{1}{6} \frac{\hat{t}^2 + \hat{u}^2}{\hat{t}\hat{u}} - \frac{3\hat{t}^2 + \hat{u}^2}{8\hat{s}^2} \right]$
$q\bar{q} \rightarrow q'\bar{q}'$	$\frac{1}{2\hat{s}} \frac{4\hat{t}^2 + \hat{u}^2}{9\hat{s}^2}$	$gq \rightarrow gq$	$\frac{1}{2\hat{s}} \left[-\frac{4\hat{s}^2 + \hat{u}^2}{9\hat{s}\hat{u}} + \frac{\hat{u}^2 + \hat{s}^2}{\hat{t}^2} \right]$
$q\bar{q} \rightarrow q\bar{q}$	$\frac{1}{2\hat{s}} \left[\frac{4}{9} \left(\frac{\hat{s}^2 + \hat{u}^2}{\hat{t}^2} + \frac{\hat{t}^2 + \hat{u}^2}{\hat{s}^2} \right) - \frac{8\hat{u}^2}{27\hat{s}\hat{t}} \right]$	$gg \rightarrow gg$	$\frac{1}{2\hat{s}} \frac{1}{2\hat{s}} \frac{9}{2} \left(3 - \frac{\hat{t}\hat{u}}{\hat{s}^2} - \frac{\hat{s}\hat{u}}{\hat{t}^2} - \frac{\hat{s}\hat{t}}{\hat{u}^2} \right)$

Figure 10: The elastic parton-parton scattering within the LO QCD, the wavy line means the gluon, whereas the solid line means the quark or antiquark(top). The differential parton-parton cross section calculated within the LO QCD (middle and bottom) [50]

- [10] A. I. Veselov, O. I. Piskunova, K. A. Ter-Martirosian, Phys.Lett. B**158** (1985) 175.
- [11] G.I.Lykasov, M.N.Sergeenko, Z.Phys.C**56**,697 (1992) *ibid* Z.Phys., C**52**,635 (1991); *ibid* Z.Phys.C**70**,455 (1996).
- [12] G.I.Lykasov, G.G.Arakelyan, M.N.Sergeenko, EPAN,v.30,p.817 (1999).
- [13] G. Watt, A.D. Martin and M.G. Ryskin, Eur.Phys.J., C **31** (2003) 73 [arXiv:hep-ph/0306169]; *ibid* Phys.Rev. D **70** (2004) 014012 [Erratum-*ibid*. D **70** (2004) 079902] [arXiv:hep-ph/0309096].
- [14] I. P. Ivanov, N. N. Nikolaev, Phys.Rev. D**65** (2002) 054004.

- [15] A. D. Martin, M.G. Ryskin and G. Watt, Eur.Phys.J., C **66** (2010) 163 [arXiv:hep-ph/0909.5529].
- [16] V.N. Gribov and L.N. Lipatov, Sov.J.Nucl.Phys. 15 (1972) 438; G. Altarelli and G. Parisi, Nucl.Phys. B 126 (1997) 298; Yu.L. Dokshitzer, Sov.Phys. JETP **46** (1977) 641.
- [17] M.A.Shifman, A.I.Vanstein, V.I.Zacharov, Nucl.Phys., B**147** (1979) 385; *ibid* B**147** (1979) 448.
- [18] S.V.Mikhailov, A.V.Radyushkin, Sov.J.Nucl.Phys., **49** (1989) 494; *ibid* Phys.Rev. D**45** (1992) 1754.
- [19] A.E.Dorokhov, S.V.Eseibegyan, S.V.Mikhailov, Phys.Rev. D**56** (1996) 4062; arXiv:9702417 [hep-ph] (1997).
- [20] T. Schaefer and E.V. Shuryak, Rev.Mod.Phys., **70** (1998) 1323.
- [21] D.Diakonov, Prog.Part.Nucl.Phys., **51** (2003) 173.
- [22] N.I. Kochelev, Phys.Lett., B**426** (1998) 149; *ibid* [arXiv:he-ph/0907.35555].
- [23] A.B.Kaidalov, Z.Phys., **C12**, 63 (1982); Sarveys High Energy Phys., **13**, 265 (1999). A.B.Kaidalov, O.I.Piskunova, Z.Phys., **C30**, 145 (1986); Yad.Fiz.,**43**, 1545 (1986).
- [24] K.A.Ter-Martitosyan, Phys.Lett., 44**B**, 377 (1973).
- [25] M.N.Sergeenko, Phys.Rev., D**61**, 03060XX (2000).
- [26] G.I. Lykasov, Z.M. Karpova, M.N. Sergeenko and V.A. Bednyakov, Europhys.Lett. **86** 61001 (2009); arXiv:hep-ph/0812.3220]
- [27] G.I. Lykasov, V.V. Lyubushkin and V.A. Bednyakov, Nucl. Phys.[Proc. Suppl.] **198** (2010) 165 [arXiv:hep-ph/0909.5061].
- [28] V.A. Bednyakov, G.I. Lykasov and V.V. Lyubushkin, Europhys.Lett. **92** (2010) 31001; arXiv:hep-ph/1005.0559.
- [29] H. Jung, Proc. of the DIS'2004, Strbaske' Pleso, Slovakia, arXiv:0411287 [hep-ph].
- [30] M.Hansson and H.Jung, arXiv:0707.4276 [hep-ph].
- [31] L.D.McLerran and R.Venugopalan, Phys.Rev D**49** (1994) 2233, arXiv:9309289 [hep-ph]; *ibid* Phys.Rev D**49** (1994) 335, arXiv:9311205 [hep-ph]; *ibid* Phys.Rev D**50** (1994) 2225, arXiv:940335 [hep-ph].
- [32] K.Golec-Biernat, M.Wusthof, Phys.Rev D**60** (1999) 114023.

- [33] J.Jalilian-Marian and Yu.V.Kovchegov, Prog.Part.Nucl.Phys.**56** (2006) 104; arXiv:0505052 [hep-ph].
- [34] V.Abramovsky, V.N.Gribov, O.Koncheli, Sov.J.Nucl.Phys., **18** (1973) 308 .
- [35] ISR Collaboration, B.Alper, et al., Nucl.Phys.,**100B**, (1975) 237.
- [36] UA1 Collaboration, C.Albajar, et al., Nucl.Phys., **B 335** , (1990) 261.
- [37] CDF Colalaboration, F.Abe, et al., Phys.Rev.Lett., **61**, (1988) 1819; ANL-HEP-PR-88-32, CDF-MEMO-MIN-BIAS-GROUP-576-August 1988.
- [38] CMS Collaboration, Vadrán Kachatryan, et al., Phys.Rev.Lett., **105**, 022002 (2010); arXiv:1005.3299 [hep-ex]; CMS-QCD-10-006, CERN-PH-EP-2010-009; FERMILAB-PUB-10-170-CMS, May 2010; *ibid* JHEP, **1002**, 041 (2010); arXiv:1002.0621 [hep-ex]; CMS-QCD, CERN-PH-EP-2010-003, Feb.2010.
- [39] ATLAS Collaboration, Georges Aad, et al., submitted to New J.Phys., arXiv:1012.5104.
- [40] Yu. M. Shabelsky, Yad. Fiz., **56**, 2512 (1992).
- [41] Piskunova O.I., Yad. Fiz., **56**, 176 (1993); **64**, 392 (2001).
- [42] O.Benhar, S.Fantoni, G.I.Lykasov, Eur.Phys.J., **A7**,415 (2000); arXiv:9901053 [hep-ph].
- [43] A. B. Kaidalov, O. I. Piskunova, Yad.Fiz., **41** (1985) 1278.
- [44] G. H. Araklyan, C. Merino, Yu. M. Shabelsky, arXiv:0604103 [hep-ph].
- [45] A.V.Efremov, Sov.J.Nucl.Phys., **19**, 176 (1974).
- [46] P.Nasson, S.Dawson & R.K.Ellis, Nucl.Phys., **B303**, 607 (1988); **B327**, 49 (1989);**B3335**, 260(E) (1989)
- [47] R.D.Field,R.P.Feyman, Phys.Rev.D **15** (1977) 2590.
- [48] R.P.Feyman, R.D.Field, and G.C.Fox, Nucl.Phys.B **128** (1977) 1.
- [49] R.P.Feyman, R.D.Field, and G.C.Fox, Phys.Rev.D **18** (1977) 3320.
- [50] M.L.Mangano, Physics-Uspekhi, **53** (2010) 109.
- [51] J.Pumplin, O.R.Stump, J.Huston, H.L.Lui, P.Nadolsky, W.K.Tung (CTEQ6L1), JHEP, **0207** (2002) 012; ArXiv:0201195 [hep-ph].
- [52] A.Sherstner, R.Torne, Eur.Phys.J **C55** (2008) 553.
- [53] S.Albino, B.A.Kniehl, G.Kramer, Nucl.Phys. **B803** (2008) 42.

